Project Report: Mass and Wind

Steven Sivek

May 10, 2005

Abstract

This report examines the effect of several geostrophically balanced forces on wind and on motion in rotating frames of reference such as the Earth. It explains experimental data demonstrating the Coriolis force and its effect on friction, providing the necessary theory to explain the obtained results, and demonstrates these ideas in practice with an analysis of atmospheric wind data.

1 Introduction

Two forces, the Coriolis force and centrifugal force, are necessary to explain the behavior of masses moving freely in a frame of reference which rotates at constant speed. In particular, the Coriolis force can be studied in isolation to determine its relation to the pressure gradient force in the Earth's atmosphere, among other forces, and hence its role in determining the wind field both with and without significant frictional forces. The following sections will try to analyze interesting consequences of the Coriolis force in both idealized and atmospheric settings and investigate its interaction with other forces such as friction.

2 Experiment: Inertial Circles

The goal of this experiment was to demonstrate the Coriolis effect on a ball bearing in a rotating frame. A nearly frictionless bearing was placed on a parabolic table rotating at such a speed that the centrifugal force and gravity on the ball cancelled each other out, leaving the ball at rest in the rotating frame of the table. The ball bearing was then deflected radially inward toward the center of the table while a rotating camera above captured its motion in the rotating frame of reference. This motion was tracked using software to empirically verify the theory that in the rotating frame, the ball bearing would follow a circular path as the Coriolis force deflected its motion rightward.

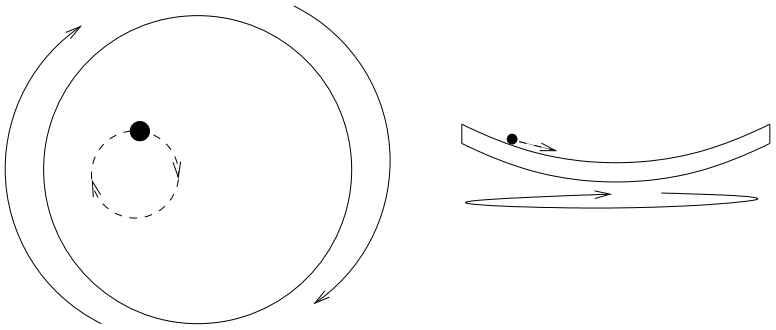

Figure 1: Top and side views of the rotating parabolic table used in the experiment.

2.1 Theory

Imagine a mass moving in a parabolic frame rotating with angular velocity $\mathbf{\Omega}$, in which the mass has position $\mathbf{r}$ relative to the center and velocities $\mathbf{u}_{in}$ and $\mathbf{u}_{rot}$ in the inertial and rotating frames of reference, respectively. The two velocities are related by $\mathbf{u}_{in} = \mathbf{u}_{rot} + \mathbf{\Omega} \times \mathbf{r}$, where the extra term is simply the rotational velocity of a point on the table itself. Hence if $\mathbf{r}$ is the position of the mass in the inertial frame, we have $\left(\frac{d\mathbf{u}_{in}}{dt}\right)_{in} = \left(\frac{d}{dt}\right)_{in} (\mathbf{u}_{rot} + \mathbf{\Omega} \times r)$. But the derivative in the inertial frame has an extra factor involving a cross product with $\mathbf{\Omega}$ to account for the rotation of the surface, so we find after some simplification that the acceleration of the mass in the inertial and rotational frames differs as follows:

$$\left(\frac{d\mathbf{u}_{in}}{dt}\right)_{in} - \left(\frac{d\mathbf{u}_{rot}}{dt}\right)_{rot} \quad = \quad (2\mathbf{\Omega} \times \mathbf{u}_{rot}) + (\mathbf{\Omega} \times \mathbf{\Omega} \times \mathbf{r})$$

If the mass is in motion in this rotating frame, and if we suppose that gravity acts on the mass as $-g\hat{\mathbf{z}}$ but friction is negligible, then we can then apply Newton's second law, $\left(\frac{d\mathbf{u}_{in}}{dt}\right)_{in} = \sum \frac{\text{force}}{\text{mass}} = -g\hat{\mathbf{z}}$, in the inertial frame to get $\left(\frac{d\mathbf{u}_{rot}}{dt}\right)_{rot} = -2\mathbf{\Omega} \times \mathbf{u}_{rot} - \mathbf{\Omega} \times \mathbf{\Omega} \times \mathbf{r} - g\hat{\mathbf{z}}$. But if the parabolic surface is stable (i.e. in a state of equilibrium) and a mass is placed on it at rest in the rotating frame, then it should be able to remain at rest there, just like the corresponding particles on the surface itself; this situation makes all terms involving $\mathbf{u}_{rot}$ in this equation equal to zero, so we conclude that $-\mathbf{\Omega} \times \mathbf{\Omega} \times \mathbf{r} - g\hat{\mathbf{z}} = 0$ and hence $\left(\frac{d\mathbf{u}_{rot}}{dt}\right)_{rot} = -2\mathbf{\Omega} \times \mathbf{u}_{rot}$.

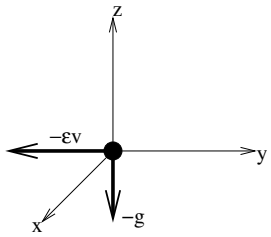

Figure 2: The forces acting on the mass if its velocity is in the y-direction.

Assuming again that the surface is more or less flat at any given point, we can break the rotational velocity into components as $\mathbf{u}_{rot} = (u, v, 0)$. Then we get the system of differential equations $\frac{du}{dt} = 2\Omega v$, $\frac{dv}{dt} = 2\Omega u$, which has solution $u(t) = A\cos(2\Omega t) + B\sin(2\Omega t)$ and $v(t) = B\cos(2\Omega t) - A\sin(2\Omega t)$ for some constants A and B. We may pick coordinates so that the initial velocity is entirely in the v-direction; if this velocity is v_0, then we have $u(t) = v_0\sin(2\Omega t)$ and $v(t) = v_0\cos(2\Omega t)$. Letting the initial coordinates of the mass within the rotating frame be (x_0, y_0), the position of the mass at time t is then $\big(x_0 + \frac{v_0}{2\Omega}(1 - \cos(2\Omega t)),\ y_0 + \frac{v_0}{2\Omega}\sin(2\Omega t)\big)$. In particular, we can conclude that the mass has constant clockwise circular motion with period $\frac{\pi}{\Omega}$, exactly half the period of rotation of the table itself (namely, $\frac{2\pi}{\Omega}$). Thus the mass completes two circular paths, each of radius $\frac{v_0}{2\Omega}$, for every complete rotation of the table.

2.2 Experimental results

The parabolic table rotated at a speed of very nearly $\Omega = \frac{\pi}{2} \approx 1.57$ radians per second, though this number varied slightly to as high as 1.6. Hence the period of the rotating frame is about 4.0 seconds.

Figure 3 displays the path of a perturbed ball moving in the rotating frame for nearly 12 seconds. The ball is seen to move in damped clockwise circles whose radii decrease very nearly linearly with time. The diameters of the outermost and innermost circles are about 0.191m and 0.0894m, respectively; these are four periods apart, so we calculate that the radius decreases by about $\frac{.191\text{m} - .0894\text{m}}{2} \approx$ .051m over the course of these four revolutions.

We can explain this decrease in radius by revising the theory of the previous section to account for friction between the ball and the table. This force should be proportional to the ball's velocity in the rotational frame, since it opposes the ball's motion, so we may quantify it as $-\epsilon\mathbf{u}_{rot}$ for some nonnegative constant ϵ. This changes the differential equation describing the motion to $\big(\frac{d\mathbf{u}_{rot}}{dt}\big)_{rot} = -2\boldsymbol{\Omega} \times \mathbf{u}_{rot} - \epsilon\mathbf{u}_{rot}$, and if we again let $\mathbf{u}_{rot} = (u, v, 0)$, then we get the system of linear first-order differential equations

$$\begin{pmatrix} u' \\ v' \end{pmatrix} = \begin{pmatrix} -\epsilon & 2\Omega \\ -2\Omega & -\epsilon \end{pmatrix} \begin{pmatrix} u \\ v \end{pmatrix}$$

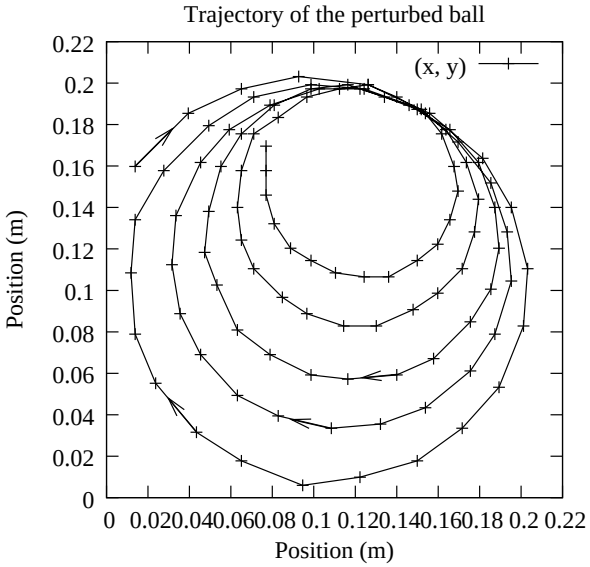

Figure 3: The trajectory of a ball perturbed toward the center of the frame.

which can be solved with some linear algebra: The eigenvalues of the coefficient matrix are $-\epsilon + 2\Omega i$ and $-\epsilon - 2\Omega i$, with eigenvectors $\begin{pmatrix} 1 \\ i \end{pmatrix}$ and $\begin{pmatrix} 1 \\ -i \end{pmatrix}$, respectively, so the solution is of the form $u(t) = Ae^{(-\epsilon+2\Omega i)t} + Be^{(-\epsilon-2\Omega i)t}$, $v(t) = Aie^{(-\epsilon+2\Omega i)t} - Bie^{(-\epsilon-2\Omega i)t}$ for some constants A and B. If we assume the coordinate axes are rotated so that $u(0) = 0$, or in other words the mass's initial motion is vertical, then we get $A + B = 0$. But the initial velocity v_o is then equal to $v(0) = 2Ai$, so we may simplify to get

$$u(t) = v_0 e^{-\epsilon t} \sin(2\Omega t), \qquad v(t) = v_0 e^{-\epsilon t} \cos(2\Omega t)$$

which has a solution of the form

$$\begin{pmatrix} x(t) \\ y(t) \end{pmatrix} = \frac{v_0 e^{-\epsilon t}}{\sqrt{\epsilon^2 + 4\Omega^2}} \begin{pmatrix} -\cos(2\Omega t - \phi) \\ \sin(2\Omega t - \phi) \end{pmatrix} + \mathbf{C}$$

for $\phi = \tan^{-1}\left(\frac{\epsilon}{2\Omega}\right)$ and some constant $\mathbf{C}$. Note that when $\epsilon = 0$, i.e. there is no friction, we also have $\phi = 0$ and this solution gives an identical result to the one derived in the friction case.

As before, we see that the mass follows a clockwise circular path with period $\frac{\pi}{\Omega}$ (half the period of the surface itself), but we note now that this path is damped by friction. Because of the damping factor $e^{-\epsilon t}$, we should expect to see the radii of these circles decrease by a constant factor of $e^{-\epsilon\pi/\Omega}$ in each period. This is equal to $e^{-k\epsilon\pi/\Omega}$ over a total of k periods, and if $\frac{\epsilon\pi}{\Omega} \ll 1$, we

may approximate this factor to first order very accurately as $1 - \left(\frac{\epsilon\pi}{\Omega}\right) k$; hence when $\frac{\epsilon\pi}{\Omega}$ is very small (as in a nearly frictionless ball bearing) the radius should decrease linearly by about $\frac{\epsilon\pi}{\Omega}$ times the original radius per period.

Letting r_0 denote the initial radius, we may estimate $\frac{4\epsilon\pi}{\Omega} r_0 \approx \frac{.191\text{m} - .0894\text{m}}{2} \approx .051\text{m}$. The motion captured in this data contains all but the first complete circle at the beginning of the ball's path, so we can assume the original radius was $r_0 \approx (.191 + \frac{1}{4}(.191 - .0894))\text{m} \approx .216\text{m}$. Since we also know $\Omega \approx \frac{\pi}{2}$, we can thus estimate the coefficient of friction: $\epsilon \approx .051\text{m} \cdot \frac{\Omega}{r_o \cdot 4\pi} \approx \frac{.051\text{m}}{.216\text{m}} \cdot \frac{1\text{s}^{-1}}{8}$, or $\epsilon \approx .0295\text{s}^{-1}$. (Note that $\epsilon\pi \ll \Omega$, so this calculation should be valid.) We can also estimate the ball's original velocity in the rotating frame from the equations of its motion: its original radius should be $\frac{v_0}{\sqrt{\epsilon^2 + 4\Omega^2}} = r_0$, so we have $v_0 = r_0\sqrt{\epsilon^2 + 4\Omega^2} = 2\Omega r_0\sqrt{1 + \left(\frac{\epsilon}{2\Omega}\right)^2} \approx 2\Omega r_0$ since $\epsilon \ll \Omega$. Therefore $v_0 \approx 2 \cdot \frac{\pi}{2} \cdot .216\text{m} = 0.68\frac{\text{m}}{\text{s}}$.

It is interesting to note in the ball's trajectory that even though the inertial circles are gradually shrinking over time, they are all tangent to a common point. The $e^{-\epsilon t}$ factor in the equations for $x(t)$ and $y(t)$ causes the path to eventually decay toward the constant point $\mathbf{C}$, so $\mathbf{C}$ must be this common point of tangency, but the equations do not suggest that the ball should repeatedly pass through or otherwise near this point rather than spiral around it. It is unclear whether this phenomenon is real or merely an interesting coincidence.

Plotting the y-coordinate of the ball's position over time as seen in Figure 4 displays this point of tangency at the local maxima, and it also shows that the radii of the circles do indeed decrease linearly over time.

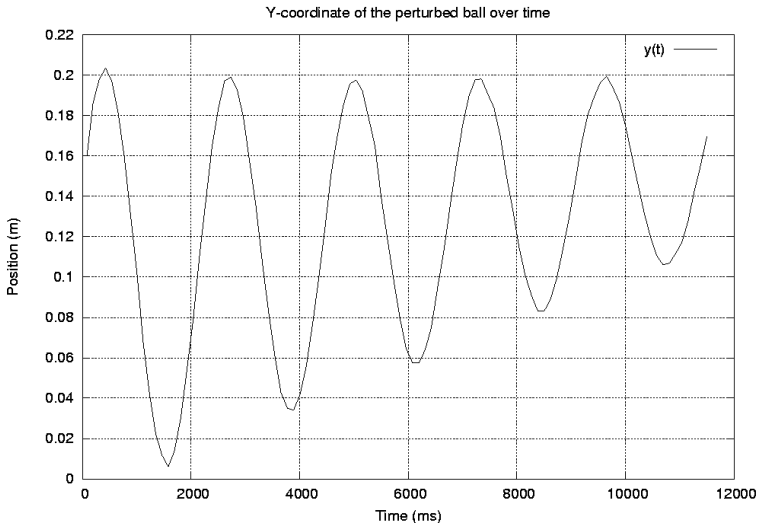

Figure 4: The y-coordinate of the ball's position over time. Note that the point of tangency is near $y = 0.2$.

The first local maximum occurs at $t = 392$ms, and the fifth occurs at $t = 9681$ms, so a quick calculation gives an average period of $\frac{9.681\text{s}-0.392\text{s}}{4} \approx 2.32$s. Given that the rotating frame has period approximately 4s, this is roughly 15% longer than the expected period of the inertial circles, 2s. It is possible that this error is due to slight inaccuracies in measuring the start and end of each period – as seen in Figure 3, the maximum y-coordinates in the ball's trajectory are achieved slightly before it passes through the point of tangency, and the delay between reaching the maximum y-coordinate and this point may vary slightly from one period to the next.

Despite this small discrepancy between the expected and actual period of the ball, we see that the theory presented here models the actual trajectory of the ball very accurately. By modeling friction as a force linearly proportional to the ball's velocity, we can estimate its period of revolution and coefficient of friction, and this theory reduces easily to a simplified version which can model inertial circles in nearly frictionless environments such as the atmosphere. We shall investigate this application in the following section.

3 Atmospheric data

Figures 5 and 6 show wind measurements above western Europe at a constant pressure of 500mb on February 15, 2005, including calculations of both the overall observed wind and the geostrophic wind. The contours mark every change of 100m in the altitude at 500mb. Furthermore, the arrows represent wind flowing from the barbs to the point of each such arrow; the barbs consist of triangles, long tick marks, and short tick marks which represent 50 m/s, 10 m/s, and 5 m/s, respectively, and may be summed to get the wind speed.

We note that in a cyclone such as the one shown over Italy, the gradient wind equation shows how the centrifugal force and Coriolis force balance the pressure gradient force:

$$\frac{v_\theta^2}{r} + f v_\theta \quad = \quad g\frac{\partial h}{\partial r}$$

where v_θ is the tangential component of the wind velocity, $f = 2\Omega \sin\phi$ is the Coriolis parameter, and h is the height at the chosen level of constant pressure. This equation applies when the Rossby number R_0 is of order unity, meaning that the ratio $\frac{v^2/r}{fv} = \frac{v}{fr}$ of the centrifugal and Coriolis forces is approximately one.

Since the data describes such high altitudes that friction is negligible, it is not surprising that the observed and geostrophic wind fields are almost identical in many places. The wind is almost entirely geostrophic, for instance, over France, where there is very little curvature in the lines of constant altitude, and indeed over the center of the country we can estimate the Rossby number to be $R_0 = \frac{v_g}{v} - 1 \approx \frac{30\ \text{m/s}}{30\ \text{m/s}} - 1 = 0$. In the cyclone centered over Italy, though, where the geostrophic wind is $v_g \approx 45\frac{\text{m}}{\text{s}}$ and the observed wind is $v \approx 25\frac{m}{s}$, we have

$R_0 = 0.8$; this is of order unity, suggesting a balance between the centrifugal force involved and the Coriolis force. Indeed, the Coriolis force acts to deflect wind outward, or away from the center of the cyclone, whereas centrifugal force pulls it back in.

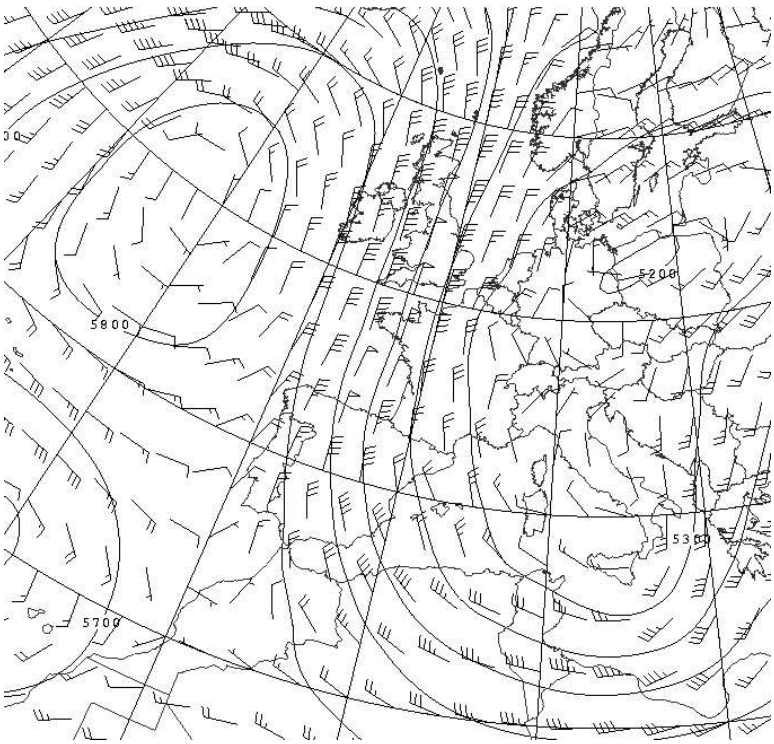

Figure 5: Observed wind over Europe at 500mb.

We can verify that the gradient wind equation, $\frac{v_\theta^2}{r} + f v_\theta = g\frac{\partial h}{\partial r}$, shows the desired balance in this case. Consider the wind near Madrid, Spain, which is moving toward the south at a speed of $v_\theta \approx 40\ \frac{\text{m}}{\text{s}}$. We estimate the latitude ϕ to be 41 degrees, so the Coriolis parameter $f = 2\Omega \sin\phi = \frac{2 \cdot 2\pi \cdot \sin(41)}{86400\text{S}} = 9.54 \cdot 10^{-5}\text{s}^{-1}$. Furthermore, the distance r to the center of the cyclone north of Sicily is about 1250 km, so $r = 1.25 \cdot 10^6\ \frac{\text{m}}{\text{s}}$, and the height contours near this point drop by $\Delta h = 300$ m over a distance of about $\Delta r = 625$ km, so we approximate $\frac{\partial h}{\partial r} = \frac{\Delta h}{\Delta r} = 4.80 \cdot 10^{-4}$.

Likewise, the observed wind one data point north of the northernmost tip of Scotland, at a latitude of 61 degrees, has a speed of $v_\theta \approx 35\ \frac{\text{m}}{\text{s}}$. Its distance r to the center of the anticyclone over the northern Atlantic Ocean is approximately 1620 km, and we estimate that the change in height is contours between these points is again 100 m over a distance of about 300 km, so $\frac{\partial h}{\partial r} \approx 3.33 \cdot 10^{-4}$.

	Cyclone (Spain)	Anticyclone (north Atlantic)
fv_θ	$3.82 \cdot 10^{-3}\ \frac{\mathrm{m}}{\mathrm{S}^2}$	$4.45 \cdot 10^{-3}\ \frac{\mathrm{m}}{\mathrm{S}^2}$
$\frac{v_\theta^2}{r}$	$1.28 \cdot 10^{-3}\ \frac{\mathrm{m}}{\mathrm{S}^2}$	$7.56 \cdot 10^{-4}\ \frac{\mathrm{m}}{\mathrm{S}^2}$
$g\frac{\partial h}{\partial r}$	$4.71 \cdot 10^{-3} \frac{\mathrm{m}}{\mathrm{S}^2}$	$3.27 \cdot 10^{-3}\ \frac{\mathrm{m}}{\mathrm{S}^2}$

Table 1: The Coriolis, centrifugal, and pressure gradient forces calculated for individual points in the cyclone and anticyclone of figures 5 and 6.

For the point in the cyclone, the left hand side of the equation (i.e. the sum of the Coriolis and centrifugal forces) is $5.10 \cdot 10^{-3}\ \frac{\mathrm{m}}{\mathrm{S}^2}$. This exceeds the calculated pressure gradient force by less than 10 percent, which is about as much accuracy as we can expect given the imprecise estimates of distance and wind speed; thus we conclude that the centrifugal and Coriolis forces do indeed balance the pressure gradient force here. In fact, the left hand side appears to be the more accurate of the two, since the geostrophic wind is given as $50\frac{\mathrm{m}}{\mathrm{S}}$ in Figure 6.

In the anticyclone, we note that the Coriolis force is oriented toward the center of the system while both the pressure gradient and centrifugal forces oppose it, so we should actually have $fv_\theta = \frac{v_\theta^2}{r} + g\frac{\partial h}{\partial r}$. In fact, the right hand side is approximately $4.03 \cdot 10^{-3}\ \frac{\mathrm{m}}{\mathrm{S}^2}$, which is less than 10 percent below the calculated Coriolis force; therefore the forces are in balance as expected.

If we instead consider the wind at much lower altitudes, such as those corresponding to 1000mb near the Earth's surface, we will see that friction has a significant effect on the Coriolis force and thus introduces a significant ageostrophic component to the wind. The reason for this is that friction between the air mass and the ground slows rotation of the air mass. The Coriolis force and the centrifugal force, both of which should push the wind away from the center of a cyclone, are proportional to the velocity and the square of the velocity of the wind around the center, respectively. Both of these forces, especially the Coriolis force since $R_0 \approx 1$ in a cyclone, are necessary to balance the pressure gradient force, however. Therefore when these forces are weakened the pressure gradient force adds a significant ageostrophic component to the wind pointing down the pressure gradient. The wind in Figure 7 illustrates this point by spiraling inward toward the center of the system, since it is flowing down the pressure gradient to the low-pressure center of the cyclone.

The observed wind in the center of Figure 7 flows eastward across the visible contours, toward the cyclone, even though the geostrophic wind should flow along those same contours. Since the pressure gradient is stronger than both of the geostrophic forces opposing it, there is a net movement of air into the cyclone at low altitudes. As the air column is pushed upward by this flow, the pressure gradient causes it to move outward at high altitudes until it is far enough away to fall back down and continue cycling in this manner.

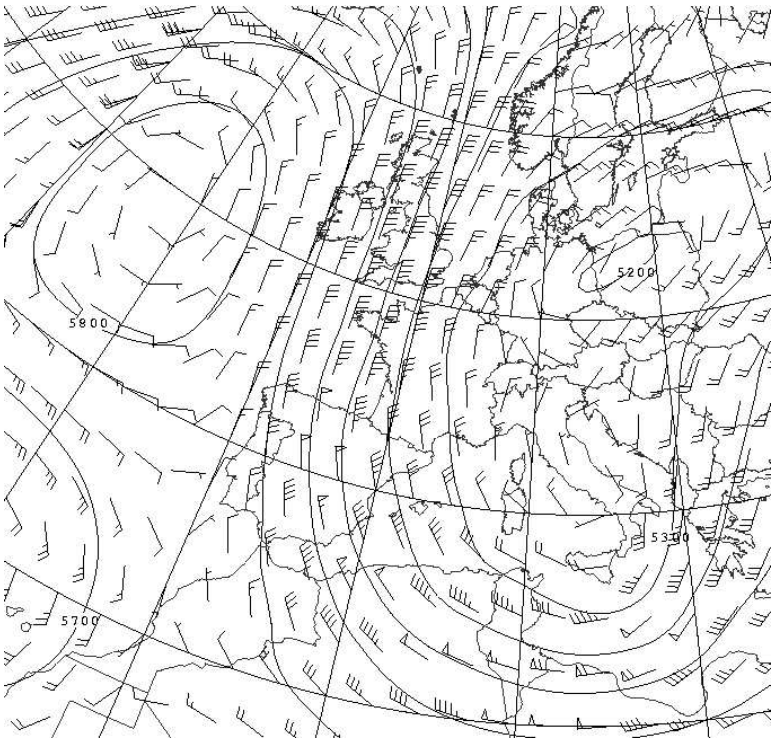

Figure 6: Geostrophic wind over Europe at 500mb.

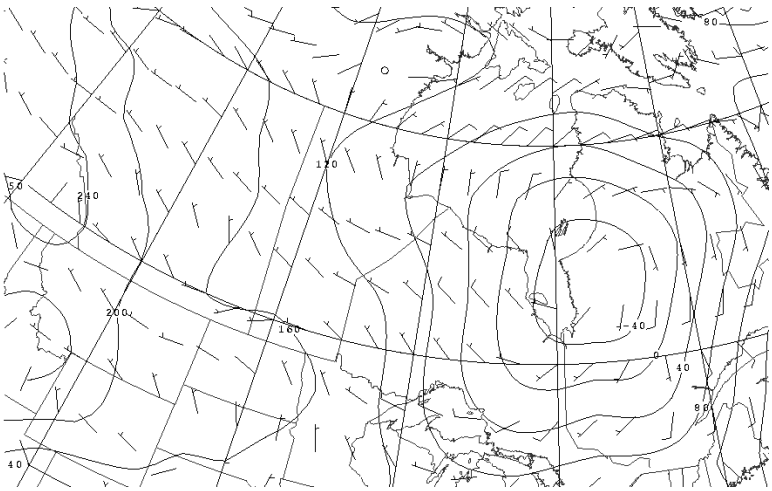

Figure 7: Observed wind over Canada at 1000mb.

If the system in question were actually a low-altitude anticyclone, then the Coriolis force would be directed inward, so it would be expected to balance both centrifugal force and the pressure gradient force. The wind would then flow away from the cyclone, since at low altitudes friction would weaken this inward force and thus push air outward. Therefore the same effect in an anticyclone would produce wind spiraling away from the center, rather than toward it as in the cyclonic case.

4 Comparing experimental and atmospheric data

The experimental data provides a simple demonstration of the Coriolis effect in a rotating frame (namely, a parabolic table). In a frictionless environment, comparable to the atmosphere at 500mb, a perturbed mass would appear to rotate indefinitely in a clockwise circular orbit relative to the rotating frame. The ball bearing used to collect this data was not frictionless, however, so the result is that the circles shrink linearly as the ball spirals inward. This can be precisely modeled with the assumption that fraction is proportional to velocity, and as such the friction can even be precisely measured.

In the lower regions of the atmosphere, friction has a similar effect on the Coriolis force, causing wind to flow inward in cyclones. Air cannot spiral inward unobstructed, since it must displace the air mass already in the center, so this effect causes rising air and hence a region of low pressure in the center of the spiral path. Therefore a pronounced pressure gradient exists, and so the Coriolis force and opposing drag force (i.e. friction) are not the only forces acting on the mass of air. Since wind is subject to many other influential forces, we cannot state any of its properties so clearly.

This is one of the most striking differences between the experimental data and the atmospheric data: The experiment is constructed in such a way that forces such as a gravity are intentionally eliminated, but in the real world, where the mass in question acts as a fluid, gravity is a necessary influence in the form of a pressure gradient force. It is therefore much harder to isolate the Coriolis force in practice, even though it can be theoretically calculated and then observed in its noticeable effect (often coupled with friction) on cyclones and anticyclones in the atmosphere. The experiment serves as an ideal way to study its theoretical properties so that it may be practically observed in real world data.

5 Conclusion

The Coriolis force causes moving bodies in a rotating frame of reference to adopt a circular path by deflecting them at right angles to their current motion and causing an angular velocity twice that of their reference frame. In the Earth's atmosphere, this force of deflection counterbalances the pressure gradient force and thus often causes the wind to move in curved paths resembling circular arcs. Just as a ball rolling along a rotating table is slowed by friction, however, the ef-

fect of friction on rotating masses of air at low altitudes is to weaken the Coriolis force and thus upset this balance. The Coriolis force is therefore responsible not just for circular wind patterns in the atmosphere but for the spiralling motion of masses such as wind into or away from cyclones and anticyclones, and thus the creation of low and high pressure systems and interesting wind phenomena within each of these systems.

References

[1] Marshall, John. "Inertial circles - visualizing the Coriolis force: GFD VI."

[2] Marshall, John and Alan Plumb. "Chapter 6: The equations of fluid motion." Available at http://www-paoc.mit.edu/labweb/notes/notes_03.htm.